ARTICLE OPEN

Check for updates

Experimental signature of initial quantum coherence on entropy production

Santiago Hernández-Gómez [ID][1,2,3,4,11 ✉], Stefano Gherardini [ID][1,5,11], Alessio Belenchia [ID][6,7,11], Andrea Trombettoni[8,9,10], Mauro Paternostro [ID][7] and Nicole Fabbri [ID][1,3]

We report on the experimental quantification of the contribution to non-equilibrium entropy production stemming from the quantum coherence content in the initial state of a qubit exposed to both coherent driving and dissipation. Our experimental demonstration builds on the exquisite experimental control of the spin state of a nitrogen-vacancy defect in diamond and is underpinned, theoretically, by the formulation of a generalized fluctuation theorem designed to track the effects of quantum coherence. Our results provide significant evidence of the possibility to pinpoint the genuinely quantum mechanical contributions to the thermodynamics of non-equilibrium quantum processes in an open quantum systems scenario.

INTRODUCTION

The irreversible character of most physical processes is, apparently, at odds with the inherent reversibility of the fundamental laws of physics. The way time-reversible quantum laws, which governs the interactions of microscopic systems, gives rise to the irreversible nature of macroscopic phenomena is a very open field of investigation[1]. In this regard, a breakthrough has been provided by the extension of the second law of thermodynamics into the quantum realm through the so-called fluctuation theorems[2–5]. A celebrated instance of this is the integral fluctuation theorem, which stems from Jarzynski's identity[2] and Crooks' relation[3], and connects the non-equilibrium energy fluctuation statistics of unital processes with the corresponding free-energy changes. Operationally, the standard approach to the quantification of energy and entropy fluctuations in non-equilibrium contexts is by using the celebrated two-point measurement (TPM) scheme[6], which requires two projective measurements, at the beginning and at the end of the dynamical process under scrutiny[7,8].

Despite the clear success of the TPM scheme, evidenced by successful experimental verification in nuclear magnetic resonance[9,10], trapped-ion[11–13], superconducting-qubit[14], nitrogen-vacancy (NV) centres[15,16] and linear optics settings[17–19], the scheme has significant limitations when considering the role played by quantum features in the statistics of energy fluctuations. In fact, any quantum coherence in the initial state of the quantum system, and expressed in the measurement basis, is washed away. As a result, the system dynamics following the first measurement is strongly affected. This has motivated recent efforts aimed at modifying the TPM scheme to take into account the presence of quantum features, particularly coherence, in non-equilibrium processes[20–33]. Ref. [34] introduced an end-point measurement (EPM) approach, where the initial statistics of energy-change fluctuations is inferred from the knowledge of the initial state and the Hamiltonian of the quantum system.

Here, we show the intrinsic operational nature of the EPM approach by considering both the detailed and the integral form of the corresponding fluctuation theorem, and using them to characterise experimentally the entropy production associated to quantum coherence in the state of an open quantum system. In particular, we experimentally make use of a qubit encoded in the spin of an NV centre in diamond, subjected to both a continuous driving and environmental effects[15,16,35]. In our experiments, we observe a significant increase of the irreversibility of the resulting dissipative map that only originates from the presence of quantum coherence in the initial state of the NV centre. Remarkably, we show that measuring such a quantity provides a tight bound for the average heat exchanged by the system with the environment.

While being valid in principle for arbitrary dynamics, our results establish NV centres as valuable platforms for the exploration of energetics at the quantum level, thus enlarging the already prominent domain of their applications in quantum technologies[36–39].

RESULTS

EPM-based fluctuation theorem

In order to set the stage for the derivation of a generalized fluctuation theorem accounting for the effects of quantum coherence of the initial state, we briefly review the EPM scheme introduced in ref. [34]. The results we provide in what follows hold for a generic open quantum system, and we thus consider an arbitrary completely-positive trace preserving (CPTP) map Φ. Let $\rho_0 = \mathcal{P} + \chi$ be the initial state of the system, which we have decomposed in its diagonal part $\mathcal{P}$ (expressed in the basis of the initial Hamiltonian $H_{t_{in}}$) and the traceless component χ that accounts for the quantum coherence. The EPM scheme prescribes to perform a single energy measurement, at the end of the

[1]European Laboratory for Non-linear Spectroscopy (LENS), Università di Firenze, Sesto Fiorentino I-50019, Italy. [2]Dipartimento di Fisica e Astronomia, Università di Firenze, Sesto Fiorentino I-50019, Italy. [3]Istituto Nazionale di Ottica del Consiglio Nazionale delle Ricerche (CNR-INO), Sesto Fiorentino I-50019, Italy. [4]Research Laboratory of Electronics, Massachusetts Institute of Technology, Street, Cambridge 02139 MA, USA. [5]Istituto Nazionale di Ottica del Consiglio Nazionale delle Ricerche (CNR-INO), Area Science Park, Basovizza I-34149 Trieste, Italy. [6]Institut für Theoretische Physik, Eberhard-Karls-Universität Tübingen, Tübingen 72076, Germany. [7]School of Mathematics and Physics, Queen's University Belfast, Belfast BT7 1NN, United Kingdom. [8]Department of Physics, University of Trieste, Strada Costiera 11, Trieste I-34151, Italy. [9]SISSA and INFN, Sezione di Trieste, Via Bonomea 265, Trieste I-34136, Italy. [10]CNR-IOM DEMOCRITOS Simulation Center, Via Bonomea 265, Trieste I-34136, Italy. [11]These authors contributed equally: Santiago Hernández-Gómez, Stefano Gherardini, Alessio Belenchia. ✉email: shergom@mit.edu

process, and to associate to it the stochastic variables $\Delta E_{i,f} \equiv E_f^{\text{fin}} - E_i^{\text{in}}$ that encodes the energy fluctuations during the open dynamics. Here, $E_k^{\text{in(fin)}}$ denotes the eigenvalues of the initial (final) Hamiltonian. We thus introduce the probability distribution $P_{\text{EPM}}(\Delta E) = \sum_{i,f} P_\Gamma(i,f)\delta(\Delta E - \Delta E_{i,f})$ for the EPM scheme, where $\delta(\cdot)$ denotes the Dirac delta function and $P_\Gamma(i,f)$ are the joint probabilities of the energy-change in the forward trajectory Γ, defined as

$$P_\Gamma(i,f) \equiv p(E_i^{\text{in}})p(E_f^{\text{fin}}) = \text{tr}(\Pi_i^{\text{in}}\rho_0)\text{tr}(\Pi_f^{\text{fin}}\Phi(\rho_0)). \quad (1)$$

Here $\Pi_j^{\text{in(fin)}}$ is the projector on the j-th initial (final) energy eigenstate. Computing the characteristic function of the probability distribution $P_{\text{EPM}}(\Delta E)$ leads immediately to an integral fluctuation relation. In fact, let us take the diagonal part $\mathcal{P}$ of the initial state ρ_0 as the thermal state of the initial Hamiltonian $H_{t_{\text{in}}}$ with inverse temperature β. One can then show that

$$\langle e^{-\beta(\Delta E - \Delta F)}\rangle = d\left[\text{tr}(\rho_{\text{th}}^{\text{fin}}\Phi(\rho_{\text{th}}^{\text{in}})) + \text{tr}(\rho_{\text{th}}^{\text{fin}}\Phi(\chi))\right], \quad (2)$$

where $\rho_{\text{th}}^{\text{fin/in}} \equiv e^{-\beta H_{t_{\text{fin/in}}}}/Z_{\text{fin/in}}$ with $Z_{\text{fin/in}} \equiv \text{tr}(e^{-\beta H_{t_{\text{fin/in}}}})$, and d is the dimension of the system's Hilbert space. The second term in the right-hand-side of Eq. (2) showcases the contribution coming from the initial quantum coherence, while the first term represents a classical deviation from the Jarzynski's equality. Such deviation would be present also in the absence of initial coherence due to the non-linearity of the EPM's probability distribution for convex combination of states[34]. Notice that the non-linearity of the probability distribution stems from enforcing the positivity and reality of the joint distribution $P_\Gamma(i,f)$ in the case the initial state and the quantum system Hamiltonian are not commuting[31,32].

Consider now an open quantum map Φ that admits a non-singular fixed point $\rho^* = \Phi(\rho^*)$. Using the results in[40], we can define the corresponding backwards dynamics (cf. *Methods – Derivation of the detailed fluctuation theorem*). In this way, one can compare the joint probabilities $P_\Gamma(i,f) = p(E_i^{\text{in}})p(E_f^{\text{fin}}) \equiv p_i^{\text{in}}p_f^{\text{fin}}$ and $P_{\widetilde{\Gamma}}(f,i) = \text{tr}(\Pi_f^{\text{fin}}\rho_B^{\text{in}})\text{tr}(\Pi_i^{\text{in}}\widetilde{\Phi}(\rho_B^{\text{in}})) \equiv \widetilde{p}_f^{\text{in}}\widetilde{p}_i^{\text{fin}}$ for measuring the energy of the quantum system in the forward and backward trajectories, Γ and $\widetilde{\Gamma}$ respectively. Notice that, in $P_{\widetilde{\Gamma}}(f,i)$, ρ_{in}^B denotes the initial state of $\widetilde{\Gamma}$, and $\widetilde{\Phi}$ is the corresponding time-reversed map.

By extending the derivation of the Jarzynski equality[2] by means of the Crooks' formalism[3,40], we consider the case in which (i) the initial quantum state of the forward dynamics is $\rho_0 = \rho_{\text{th}}^{\text{in}} + \chi$, i.e., ρ_0 is written as the sum of a thermal state at inverse temperature β and the traceless component χ encoding the initial coherence in the energy basis, and (ii) the initial state of the backward quantum dynamics is the state that is thermal in the final Hamiltonian at the same inverse temperature β of the forward process, i.e., $\rho_B^{\text{in}} = Z_{\text{fin}}^{-1}\exp[-\beta H_{t_{\text{fin}}}] = \rho_{\text{th}}^{\text{fin}}$. These assumptions allow to write the balance equation

$$\frac{P_\Gamma(i,f)}{P_{\widetilde{\Gamma}}(f,i)} = \exp\left[\beta(\Delta E_{i,f} - \Delta F) + \Delta\sigma_{i,f} + \Delta\Sigma_{i,f}\right], \quad (3)$$

where

$$\Delta\sigma_{i,f} \equiv \ln\frac{p_f^{\text{fin}}(\rho_{\text{th}}^{\text{in}})}{\widetilde{p}_i^{\text{fin}}(\rho_B^{\text{in}})}, \qquad \Delta\Sigma_{i,f} \equiv \ln\left[1 + \frac{p_f^{\text{fin}}(\chi)}{p_f^{\text{fin}}(\rho_{\text{th}}^{\text{in}})}\right] \quad (4)$$

and $p_f^{\text{fin}}(\chi) \equiv \text{tr}(\Pi_f^{\text{fin}}\Phi(\chi))$ (cf. *Methods – Derivation of the detailed fluctuation theorem*). Accordingly, averaging Eq. (3) over the forward probability distribution, one obtains

$$\left\langle e^{-\beta\Delta E - (\Delta\sigma + \Delta\Sigma)}\right\rangle_\Gamma = e^{-\beta\Delta F}. \quad (5)$$

Eq. (3) and Eq. (5) are the *detailed* and the *integral* forms of the EPM's fluctuation theorem, respectively.

It is worth noting that, by construction, $p_f^{\text{fin}}(\chi)$ can be negative as it operates on the quantum coherence operator χ, which is Hermitian but traceless. However, the quantity $\Delta\Sigma_{i,f}$ is well-defined, as the term inside the logarithm is always non-negative. In fact, $p_f^{\text{fin}}(\rho_{\text{th}}^{\text{in}}) + p_f^{\text{fin}}(\chi) = p_f^{\text{fin}}(\rho_0) \geq 0$. In addition, thanks to the assumption (ii), $\Delta\Sigma_{i,f}$ depends only on the forward dynamics and it satisfies a fluctuation theorem by its own (cf. *Methods – Derivation of the integral fluctuation theorem*), i.e.,

$$\left\langle e^{-\Delta\Sigma}\right\rangle_\Gamma = 1. \quad (6)$$

Resorting to the Jensen's inequality, one has $\langle\Delta\Sigma\rangle \geq 0$. $\Delta\Sigma$ encodes the entropic contribution of the initial quantum coherence of the system, and we thus identify it as the *coherence-affected irreversible entropy production* for a non-equilibrium dynamical process. At the same time, the quantity $\Delta\sigma$ represents a completely classical contribution to the entropy production that comes from adopting the EPM formalism, namely from the extra uncertainty implied by the factorization condition in Eq. (1) (see also discussion in ref. [34]).

The experimental system

We consider the spin qubit associated to a negatively charged NV centre –a localized impurity in a diamond lattice based on a nitrogen substitutional atom next to a vacancy– which forms an electronic spin $S = 1$ in its orbital ground state[41–44]. A magnetic bias field aligned with S_z removes the degeneracy of the spin eigenstates, so as to allow for the selective coherent manipulation of the transition $|S_z = 0\rangle \leftrightarrow |S_z = +1\rangle$. The Hamiltonian H of this effective two-level system is determined by a continuous nearly resonant microwave field and, in the frame rotating at the microwave frequency, the Hamiltonian is $H = \hbar\omega(\cos\alpha\,\tilde{\sigma}_z - \sin\alpha\,\tilde{\sigma}_x)/2$, where $\omega = \sqrt{\Omega^2 + \delta^2}$ and $\tan\alpha = -\Omega/\delta$; Ω denotes the bare Rabi frequency and $\delta \in [0, \Omega]$ is the microwave detuning. We have used the tilde for the Pauli matrices in view of the change of basis to the Hamiltonian eigenstates, i.e., $\{|0\rangle, |1\rangle\} \equiv \{\cos\frac{\alpha}{2}|S_z = 0\rangle - \sin\frac{\alpha}{2}|S_z = +1\rangle, \sin\frac{\alpha}{2}|S_z = 0\rangle + \cos\frac{\alpha}{2}|S_z = +1\rangle\}$ with eigenvalues $\pm\hbar\omega/2$. In this new basis, the Hamiltonian becomes $H = \omega\sigma_z/2$, where $\hbar$ is set to 1 from here on.

The qubit is governed by an alternated sequence of unitary and non-unitary (controlled-dissipative) dynamics, as follows. The system is repeatedly subjected to a sequence of pulses, occurring regularly at time intervals τ. Among two consecutive pulses, the evolution of the NV centre is unitary and described by the operator $U \equiv \exp[-iH\tau]$. As depicted in Fig. 1, the NV spin also undergoes open dynamics due to
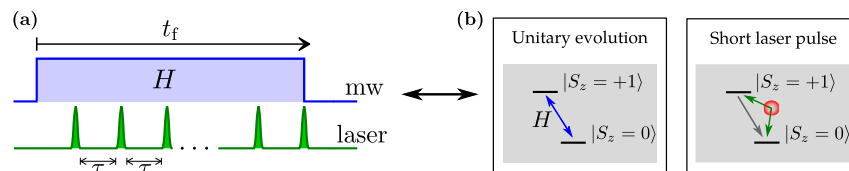

Fig. 1 Scheme of the protocol applied to the NV spin qubit. The dynamics stems from a combination of coherent driving of the qubit (near-resonance microwave (mw) radiation) and a train of short laser pulses that makes "open" the system (**a**). Specifically, the coherent drive couples the states $|S_z = 0\rangle$ and $|S_z = +1\rangle$. Instead, the short laser pulses act as a dissipation, by first projecting the system into the S_z eigenstates and then optically pumping part of the populations towards the $|S_z = 0\rangle$ state (**b**).

its interaction with a train of short laser pulses with a duration t_L that is much shorter than the characteristic time-scale of the unitary dynamics ($t_L \ll 2\pi/\omega$). The short laser pulses trigger cycles of spin preserving and non-preserving transitions between different orbital levels[15,45,46]. This entails non-unitary dynamics that project the state of the system into the eigenstates of $\tilde{\sigma}_z$ and partially transfer the spin population to $|S_z = 0\rangle$. Such *spin amplitude damping* along the $\tilde{\sigma}_z$ axis, also known as optical pumping, is caused by the spin non-preserving transitions, and can be modelled as a controlled dissipative channel toward $|S_z = 0\rangle$[15,35]. The overall dynamics takes the NV centre into an asymptotic fixed point ρ^* that we can use to define the backward dynamics [see Supplementary Note 1 for more details on the modelling of the NV centre dynamics in the experiment]. In the experiments shown throughout this work, we set $a = \pi/4$ (i.e., $\delta = -\Omega$), $\tau\omega \simeq (2\pi)0.9$, and $\tau = 190$ ns.

Coherence-affected entropy production

We now show the results obtained with the NV qubit subjected to the dissipative dynamics introduced above. Here, our aim is to characterize the thermodynamic role of initial quantum coherence in terms of the coherence-affected entropy production. We have thus performed a series of experiments to determine both the EPM probability distribution of energy-change fluctuations as well as the usual TPM one.

At the beginning of each experimental realization, the electronic spin is initialized into the $|S_z = 0\rangle$ eigenstate of the spin operator S_z via optical spin pumping under long laser excitation. Then, the system is brought in each of the four different pure states that correspond to the eigenvectors of σ_z and σ_y, by applying rotation gates (on-resonant microwave pulse) to the state $|S_z = 0\rangle$. After n short laser pulses, with $n \in [0, N]$, we measure the energy of the system in the Hamiltonian basis σ_z. To achieve this, we optically readout the intensity of the NV photo-luminescence (PL). The PL intensity (averaged over $\sim 10^6$ repetitions of the experiment) determines the probability for the system to be in the energy eigenstate $|1\rangle$ (see *Methods* for a more detailed description of the readout process). This approach allows us to achieve an experimental estimate of $p_{f=1}^{\text{fin}}(\rho) = \text{tr}(\Pi_{f=1}^{\text{fin}}\Phi(\rho))$, where ρ is one of the eigenstates of either σ_z or σ_y. From this, we obtain the probability for $f = 0$ as $1 - p_{f=1}^{\text{fin}}(\rho)$. As we collect data from several experiments (in which the system is initialized in one of the four pure qubit-states $\{|0\rangle, |1\rangle, |+\rangle_y, |-\rangle_y\}$), it is a matter of data processing to compute the EPM and TPM statistics for every classical mixture of such states (for more details see Supplementary Note 2). In particular, looking at a Bloch sphere representation for the qubit, this implies that we are able to obtain the statistics of the quantum process for any initial state included in the $y - z$ equatorial plane of the Bloch sphere, i.e. any initial state expressed as a convex combination of the states $|0\rangle, |1\rangle, |+\rangle_y, |-\rangle_y$. Specifically, in the following we show experimental results corresponding to the initial states (expressed in the Hamiltonian basis)

$$\rho_0 = \frac{1}{2}\begin{pmatrix} 1+p & -(1-p)i \\ (1-p)i & 1-p \end{pmatrix} \tag{7}$$

with $p \in [0,1]$, such that ρ_0 is the convex mixture of $|1\rangle\langle 1|$ and $|+\rangle_y\langle +|$ with probability p and $1 - p$, respectively. We also need to consider data associated to the state $\rho_B^{\text{in}} = \frac{1}{2}(\mathbb{1} + p\sigma_z)$. Notice that in ref. [15] we reported similar experimental results, but only considering diagonal states ρ_B^{in}. While the working point defined by the choice of experimental parameters ($\delta, \Omega, \tau, t_L$) is unique of the experiments reported here, our investigation goes significantly beyond the context set in ref. [15] in light of the fact that we have addressed the case of coherent (non-diagonal) states.

The first quantity we are interested in characterizing experimentally is the coherence-affected entropy production encoded in the average of $\Delta\Sigma$ as given in Eq. (4). Notice that this average is defined solely in terms of the forward trajectory probability; thus, we can fully characterize it by resorting to the experimental data acquired during the forward dynamics. The results of our experiments are shown in Fig. 2: in panel (a) we present the experimental values of the stochastic quantum entropy production $\Delta\Sigma_{i,f}$, and in panel (b) we show the experimental verification of the fluctuation theorem in Eq. (6). Instead, in panel (c), the behaviour of $\langle\Delta\Sigma\rangle$ is plotted as a function of the number of laser
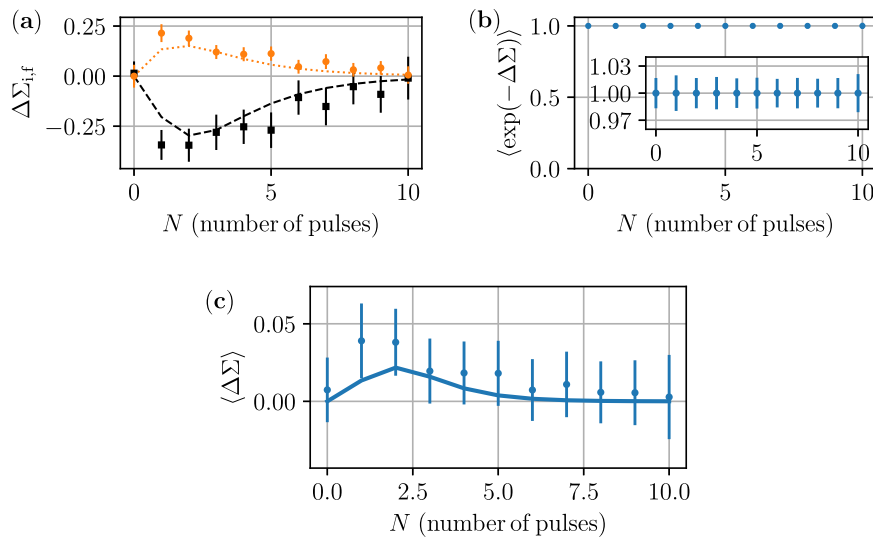

Fig. 2 Coherence-affected entropy production. a Comparison between experimental (markers with error bars) and numerical values (lines) of the coherence-affected irreversible entropy production $\Delta\Sigma_{i,f}$. Black squares and dashed line: $\Delta\Sigma_{1,1} = \Delta\Sigma_{0,1}$; orange bullets and dotted line: $\Delta\Sigma_{1,0} = \Delta\Sigma_{0,0}$. Note that these equalities stem from the fact that, given the chosen initial state of the backward quantum dynamics, $\Delta\Sigma_{i,f}$ depends only on the index f [Eq. (4)]. **b** Experimental verification of the fluctuation theorem $\langle e^{-\Delta\Sigma}\rangle_\Gamma = 1$ [Eq. (6)] as a function of the number N of pulses. Error-bars are comparable to the size of the bullets. Inset: $\langle e^{-\Delta\Sigma}\rangle_\Gamma$ in the range [0.97, 1.03]. **c** Experimental average coherence-affected entropy production as a function of N (blue circles). In all the panels, the experimental data and the numerical simulations are obtained by taking $|+\rangle_y = (|0\rangle + i|1\rangle)/\sqrt{2}$ (i.e., ρ_0 with $p = 0$) as the initial quantum state. For such an initial state, the coherence-affected entropy production is nearly extremal. Error bars correspond to propagated standard deviation of the normalized PL.

pulses. While the error bars are quite large, it can be observed how the corresponding experimental points nicely follow the theoretical predictions and how the experimental data show a positive coherence-affected entropy production.

Another quantity that can be investigated directly from the available data on the forward dynamics is the average of the energy-change fluctuations ΔE. In this regard, it is worth noting that this quantity is identified with the average work when considering time-dependent unitary processes like in the Jarzynski's original work[2]. In our case, as the Hamiltonian is time-independent, we can unambiguously interpret this quantity as the average *heat* that the system exchanges with its environment, by means of the open dynamics to which the NV centre is subjected. The average of the stochastic variable $\Delta E_{i,f} = E_f - E_i$ in the EPM approach is related to the TPM scheme via the following relation:

$$\langle \Delta E \rangle_{\text{EPM}} = \langle \Delta E \rangle_{\text{TPM}} + \sum_f \text{tr}(\Pi_f^{\text{fin}} \Phi(\chi)) E_f . \tag{8}$$

The second term on the right-hand side of Eq. (8) represents a contribution to the average heat ascribable to the quantum coherence of the initial state, which is not deleted by a first energy measurement over ρ_0. Figure 3 displays the three quantities entering in Eq. (8), by comparing theoretical expectations with the experimental results. It is shown that the experimental data are able to discern the coherence contribution to the heat exchanged between the system and the environment due to the pulsed dynamics. Among the protocols that allows to account for quantum features in energy fluctuations[20–23,27–29,31,34], the EPM scheme requires only a final energy measurement at the time t and does not require any knowledge of the quantum map Φ that models the forward dynamics. This makes the method particularly suitable for application in open quantum systems.

Finally, we have also verified the validity of the full EPM fluctuation theorem in Eq. (5) as well as its consequences for the expectation values of the involved thermodynamic quantities. In principle, this requires having access to the backward trajectories of the system, so as to characterize $\Delta \sigma_{i,f}$ in Eq. (4). This can be problematic when the system dynamics is non-unitary: while the backward trajectories can be easily simulated numerically, implementing them at the experimental level is not currently possible with our set-up. However, for the range of experimental parameters, the choice of the initial state of the backward process and the form $\tilde{\Phi}$ obtained from[40] thanks to the existence of a non-singular fixed point of the dynamics, the backward dynamics are such that $\tilde{p}_j^{\text{fin}}(\rho_B^{\text{in}}) = p_j^{\text{fin}}(\rho_{\text{th}}^{\text{in}})$. Therefore, by assuming that this property holds and thus that we can estimate $\langle \Delta \sigma \rangle$ from the sole data of the forward trajectories, in Fig. 3b we show the
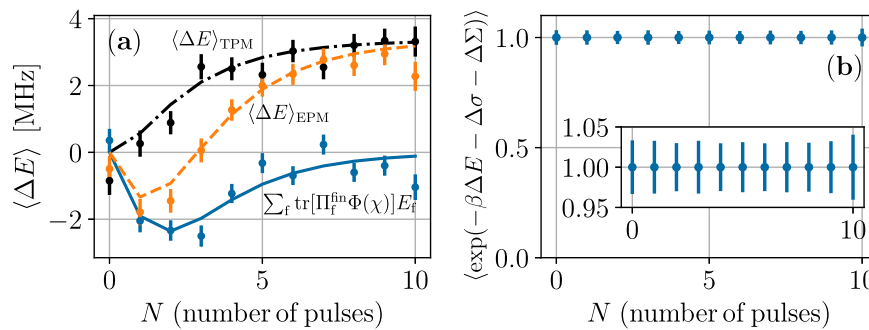
experimental verification of the integral form of the EPM fluctuation theorem in Eq. (5).

The application of the Jensen inequality to Eqs. (2) and (5) leads to

$$\beta \langle \Delta E \rangle \geq \begin{cases} -\ln(\mathcal{G}_{\text{EPM}}), \\ -(\langle \Delta \sigma \rangle + \langle \Delta \Sigma \rangle) \end{cases} \tag{9}$$

with $\mathcal{G}_{\text{EPM}} = 2\text{tr}\left(\rho_{\text{th}}^{\text{fin}} \Phi(\rho_{\text{th}}^{\text{in}} + \chi)\right)$ denoting the EPM characteristic function[34]. In Fig. 4, the theoretical expectations of these quantities are compared with the corresponding experimental results. For the initial state ρ_0 considered for this figure (i.e., the state in Eq. (7) with $p = 0.38$), the results obtained by using the characteristic function of the EPM approach are quite distinct from the ones coming from the integral fluctuation theorem (5). Specifically, for $N \in [0, 10]$ and for the initial states accessible from the experimental data, the bound on $\langle \Delta E \rangle$ derived from the integral fluctuation theorem is *tighter* than the one resulting from $\mathcal{G}_{\text{EPM}}$. In addition, we can also see in Fig. 4 that the inequality in Eq. (9) is almost saturated, meaning that the average heat exchange from the EPM method offers even a good estimate of the sum $\langle \Delta \Sigma + \Delta \sigma \rangle$ in the regime experimentally analyzed.

DISCUSSION
We have used the end-point measurement (EPM) approach for the characterization of energy-change fluctuations arising from a non-equilibrium process, with the aim to quantify the contribution to the entropy production that is originated by the presence of quantum coherence in the initial density matrix of the quantum system under scrutiny.

The results obtained from the EPM scheme have to be compared with the ones arising from the two-point measurement (TPM) scheme. While in the TPM an initial projective measurement cancels out any effect of the quantum coherence of the initial state in the basis of the measured observable, the EPM preserves such coherence. In order to compare these two schemes, in this work we followed the standard set-up of the TPM scheme while allowing for initial coherence in the energy basis applying the EPM approach. As a general remark, notice that the coherence of an initial quantum state crucially influences the system evolution, and consequently the physical quantities associated with the system dynamics, such as the quantum entropy production.

Our formalism gives a physical characterization of the entropy production associated with an arbitrary preparation of the system. Besides the quantum entropy originated during the dynamics, our results clearly single-out the presence of a change of entropy production due to the absence of the first measurement, and of an entropy production solely depending on the quantum
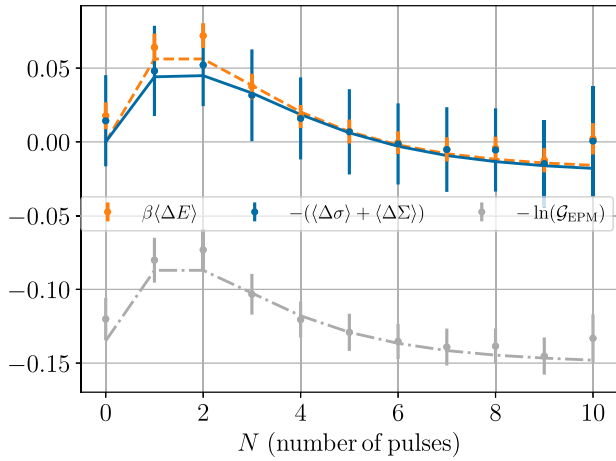

Fig. 3 Average energy-change and integral fluctuation theorem. a Shows the three quantities in Eq. (8). The dashed orange curve stands for $\langle \Delta E \rangle_{\text{EPM}}$, the dot-dashed black one for $\langle \Delta E \rangle_{\text{TPM}}$, and the solid blue line shows the contribution of quantum coherence to the *exchanged heat* $\sum_f \text{tr}(\Pi_f^{\text{fin}} \Phi(\chi)) E_f$. The curves are obtained for an initial state parameterized as in Eq. (7) with $p = 0.2$. This choice guarantees a good visibility of all the contributions. **b** Experimental verification of the integral form of the EPM fluctuation theorem in Eq. (5). In this panel, we have taken Eq. (7) with $p = 0.38$. Inset: Integral fluctuation theorem in the range [0.95, 1.05]. Error bars correspond to propagated standard deviation of the normalized PL.

Fig. 4 Jensen inequality at work: a tight bound for the averaged heat exchange. The dashed orange curve corresponds to the average heat exchange $\beta\langle\Delta E\rangle$ from the EPM method. The dot-dashed grey and solid blue curves show the behaviour of the right-hand-sides of the inequalities in Eq. (9). The initial state is taken as in Eq. (7) with $p = 0.38$.

coherence of the initial state. By focusing the attention on the latter contribution, we have shown that the EPM formalism provides –quite naturally– the fluctuation theorem for the quantum entropy production linked to the quantum coherence of the initial state.

The operational nature of our approach has enabled a successful experimental assessment of such coherence-affected entropy production in a solid state platform, at room-temperature and inherently dissipative, where an NV spin qubit is addressed by a sequence of laser pulses so that it undergoes a controlled dissipative dynamics.

Our study grounds the EPM approach as a powerful framework to assess the role of quantum coherence in the energetics of quantum systems and devices[47]. Specifically, our findings add a crucial ingredient for the analysis of the thermodynamic role of quantum coherence and allow the characterization of the introduced entropy production due to quantum coherence. It seems natural to associate the entropy production heralded by quantum coherence in the initial state, to the system dissipation. While our work has provided robust empirical and experimental evidence for this connection, further investigations are required to formalise and establish it definitively.

METHODS

Here we report a detailed derivation of the detailed and integral fluctuation theorems analyzed in the section Results.

Derivation of the detailed fluctuation theorem

Let us consider a CPTP map, written in Kraus representation as $\Phi(\bullet) = \sum_a K_a \bullet K_a^\dagger$ with $\{K_a\}$ the set of Kraus operators, that allows a non-singular fixed point ρ^* such that $\rho^* = \Phi(\rho^*)$. As ρ^* is non-singular, following Crooks' formalism[40] we can define the time-reversed map as

$$\widetilde{\Phi}(\bullet) = \sum_a [(\rho^*)^{1/2}K_a^\dagger(\rho^*)^{-1/2}] \bullet [(\rho^*)^{-1/2}K_a(\rho^*)^{1/2}], \quad (10)$$

where $\widetilde{K}_a \equiv (\rho^*)^{1/2}K_a^\dagger(\rho^*)^{-1/2}$.

Then, in accordance with the EPM formalism[34], we can introduce the expression of the joint probabilities $P_\Gamma(E_i^{in}, E_f^{fin}) \equiv P_\Gamma(i, f)$ and $P_{\widetilde{\Gamma}}(E_\ell^{fin}, E_k^{in}) \equiv P_{\widetilde{\Gamma}}(\ell, k)$, respectively, for the quantum

trajectories Γ and $\widetilde{\Gamma}$ of the forward and backward process, respectively. Let us observe that the latter is obtained by reversing the arrow of time by means of a transformation that obeys the time-reversal symmetry. Specifically, one has

$$P_\Gamma(i, f) = \mathrm{tr}(\Pi_i^{in}\rho_0)\mathrm{tr}(\Pi_f^{fin}\rho^{fin}) \equiv p_i^{in}p_f^{fin} \quad (11)$$

and

$$P_{\widetilde{\Gamma}}(\ell, k) = \mathrm{tr}(\Pi_\ell^{fin}\rho_B^{in})\mathrm{tr}(\Pi_k^{in}\rho_B^{fin}) \equiv \widetilde{p}_\ell^{in}\widetilde{p}_k^{fin} \quad (12)$$

where, we recall, $\rho^{fin} \equiv \Phi[\rho_0]$ and $\rho_B^{in} \equiv \widetilde{\Phi}[\rho_B^{in}]$ with ρ_B^{in} denoting the initial state of the backward process and, without loss of generality, we have assumed that each projector on the energy eigenstates is invariant to the application of the time-reversal transformation. As a result, the expression of the *detailed balance equation* for the trajectories Γ and $\widetilde{\Gamma}$ is formally equal to

$$\frac{P_\Gamma(i, f)}{P_{\widetilde{\Gamma}}(\ell, k)} = \frac{p_i^{in}p_f^{fin}}{\widetilde{p}_\ell^{in}\widetilde{p}_k^{fin}} . \quad (13)$$

Before proceeding, it is worth observing that if (i) we apply the EPM scheme for characterising energy-change fluctuations and (ii) we choose the initial state of the backward process as the time-reversal of the final state of the forward process, then $\widetilde{p}_\ell^{in} = p_f^{fin}$ for $\ell = f$. As a matter of fact,

$$\widetilde{p}_\ell^{in} = \mathrm{tr}(\rho_B^{in}\Pi_\ell^{fin}) = \mathrm{tr}(\Theta\rho^{fin}\Theta^\dagger\Theta\Pi_\ell^{fin}\Theta^\dagger) = \mathrm{tr}(\rho^{fin}\Pi_\ell^{fin}) = p_\ell^{fin} \quad (14)$$

where $\widetilde{(\bullet)} \equiv \Theta(\bullet)\Theta^\dagger$ with Θ denoting the time-reversal operator. The latter, by construction, is anti-unitary, i.e., it is an anti-linear operator and satisfies the relations $\Theta^\dagger\Theta = \Theta\Theta^\dagger = \mathbb{I}$. In this context, we obtain the fluctuation relation

$$\frac{P_\Gamma}{P_{\widetilde{\Gamma}}}(i, f) = e^{-\Delta\overline{\sigma}_i^{in}} \quad (15)$$

where we have identified

$$\Delta\overline{\sigma}_i^{in} = -\ln\frac{\mathrm{tr}(\rho_0\Pi_i^{in})}{\mathrm{tr}\left(\widetilde{\Phi}(\rho_B^{in})\Pi_i^{in}\right)} . \quad (16)$$

This relation encodes information only on the initial stochastic quantum entropy production due to the open system dynamics. In fact, for the special case in which the dynamics is *unitary*, and under the assumption of micro-reversibility, i.e., $\Theta\mathcal{U}(\lambda)\Theta^\dagger = \mathcal{U}^\dagger(\widetilde{\lambda})$ with $\lambda(t)$ generic time-dependent transformation such that the system Hamiltonian is invariant under time-reversal, one finds that $e^{-\Delta\overline{\sigma}_i^{in}} = 1 \ \forall i$, i.e.,

$$P_\Gamma(i, f) = P_{\widetilde{\Gamma}}(f, i) . \quad (17)$$

Notice also that, in determining the integral form of Eq. (15), one gets $\langle e^{\Delta\overline{\sigma}^{in}}\rangle_\Gamma = 1$ with

$$\langle\Delta\overline{\sigma}^{in}\rangle_\Gamma = \sum_i p_i^{in}\ln\frac{\widetilde{p}_i^{fin}}{p_i^{in}} = -S(p||\widetilde{p}), \quad (18)$$

where, we recall, p_i^{in} and $\widetilde{p}_i^{fin}$ are the probabilities to measure the i-th energy value of the system, respectively, at the initial and final time instants of the forward and backward process. Here, $S(q||p)$ is the *classical relative entropy* between the two probability distributions q and p, and thus it naturally corresponds to a measure of how far is the final state of the inverse quantum dynamics from the initial quantum state.

Coming back to the derivation of Eq. (3) in the main text, let us assume that (i) the initial quantum state ρ_0 of the forward dynamics has thermal populations but also non-zero coherence terms (in the energy basis of the system), and (ii) the initial quantum state ρ_B^{in} of the backward quantum dynamics has thermal populations (with respect to the final Hamiltonian) and

once again non-vanishing off-diagonal elements. In other terms,

$$\rho_0 = \rho_{\text{th}}^{\text{in}} + \chi^{\text{in}} \equiv \frac{e^{-\beta H_{t_{\text{in}}}}}{Z_{\text{in}}} + \chi^{\text{in}} \tag{19}$$

$$\rho_B^{\text{in}} = \rho_{\text{th}}^{\text{fin}} + \chi^{\text{fin}} \equiv \frac{e^{-\beta H_{t_{\text{fin}}}}}{Z_{\text{fin}}} + \chi^{\text{fin}}, \tag{20}$$

where $\mathrm{tr}(\chi^{\text{in}}) = \mathrm{tr}(\chi^{\text{fin}}) = 0$, $Z_{\text{fin/in}} \equiv \mathrm{tr}(\exp[-\beta H_{t_{\text{fin/in}}}])$ and the system Hamiltonian H is not necessarily assumed as a time-independent operator. Thus, by substituting Eqs. (19) and (20) into (13) with $k = i$ and $\ell = f$, one finds

$$\frac{P_\Gamma(i,f)}{P_{\tilde{\Gamma}}(f,i)} = \exp\Big[\beta(\Delta E_{i,f} - \Delta F) + \sigma_f^{\text{fin}}(\rho_{\text{th}}^{\text{in}}) + \Sigma_f^{\text{fin}}(\chi^{\text{in}}) - \tilde{\sigma}_i^{\text{fin}}(\rho_{\text{th}}^{\text{fin}}) - \tilde{\Sigma}_i^{\text{fin}}(\chi^{\text{fin}})\Big], \tag{21}$$

where

$$\sigma_f^{\text{fin}}(\rho_{\text{th}}^{\text{in}}) \equiv \ln p_f^{\text{fin}}(\rho_{\text{th}}^{\text{in}}) \tag{22}$$

$$\Sigma_f^{\text{fin}}(\chi^{\text{in}}) \equiv \ln\left(1 + \frac{p_f^{\text{fin}}(\chi^{\text{in}})}{p_f^{\text{fin}}(\rho_{\text{th}}^{\text{in}})}\right) \tag{23}$$

$$\tilde{\sigma}_i^{\text{fin}}(\rho_{\text{th}}^{\text{fin}}) \equiv \ln \tilde{p}_i^{\text{fin}}(\rho_{\text{th}}^{\text{fin}}) \tag{24}$$

$$\tilde{\Sigma}_i^{\text{fin}}(\chi^{\text{fin}}) \equiv \ln\left(1 + \frac{\tilde{p}_i^{\text{fin}}(\chi^{\text{fin}})}{\tilde{p}_i^{\text{fin}}(\rho_{\text{th}}^{\text{fin}})}\right), \tag{25}$$

$p_f^{\text{fin}}(\mathcal{A}) \equiv \mathrm{tr}(\Pi_f^{\text{fin}}\Phi(\mathcal{A}))$, and $\tilde{p}_i^{\text{fin}}(\mathcal{A}) \equiv \mathrm{tr}\left(\Pi_i^{\text{fin}}\tilde{\Phi}(\mathcal{A})\right)$ with $\mathcal{A}$ a generic linear operator. It is worth noting that $p_f^{\text{fin}}(\mathcal{A})$ and $\tilde{p}_i^{\text{fin}}(\mathcal{A})$ denote the probability to measure the f-th and i-th final energy values of the quantum system in the forward and backward process, respectively, conditioned to have evolved the thermal contribution of the initial state (without coherence terms in the energy eigenbasis). Finally, Eq. (21) can be simplified as

$$\frac{P_\Gamma(i,f)}{P_{\tilde{\Gamma}}(f,i)} = \exp\big[\beta(\Delta E_{i,f} - \Delta F) + \Delta\sigma_{i,f} + \Delta\Sigma_{i,f}\big], \tag{26}$$

by introducing the quantities

$$\Delta\sigma_{i,f} \equiv \sigma_f^{\text{fin}}(\rho_{\text{th}}^{\text{in}}) - \tilde{\sigma}_i^{\text{fin}}(\rho_{\text{th}}^{\text{fin}}) \quad \text{and} \quad \Delta\Sigma_{i,f} \equiv \Sigma_f^{\text{fin}}(\chi^{\text{in}}) - \tilde{\Sigma}_i^{\text{fin}}(\chi^{\text{fin}}). \tag{27}$$

Let us observe that, if no quantum coherence is present neither in ρ_0 nor in ρ_B^{in} (i.e., $\chi^{\text{in}} = \chi^{\text{fin}} = 0$), then $\Delta\Sigma_{i,f} = 0$. Thus, $\Delta\Sigma_{i,f}$ can be considered as a *correction*, due to initial coherence in the energy basis of the system, to the entropy difference $\Delta\sigma_{i,f}$ obtained by propagating initial thermal states in the forward and backward process, respectively.

The form of the detailed fluctuation theorem used in the main text is a particular case of Eq. (26) where χ^{fin} is assumed to be vanishing. This choice is motivated by our aim to consider the minimal modification to the "Jarzynski set-up", respect to which only coherence in the initial state of the forward dynamics is added.

Derivation of the integral fluctuation theorem for ΔΣ

From Eq. (26) the integral fluctuation theorem of Eq. (5) can be easily obtained.

Instead, for what concerns the integral fluctuation theorem involving the sole coherence induced entropy production, let us consider the case in which $\chi^{\text{fin}} = 0$. Upon substitution, one has

$$\exp[-\Delta\Sigma] = \frac{p_f^{\text{fin}}(\rho_{\text{th}}^{\text{in}})}{p_f^{\text{fin}}(\rho_{\text{th}}^{\text{in}}) + p_f^{\text{fin}}(\chi^{\text{in}})}. \tag{28}$$

Thus, taking the average over the EPM probability distribution of the forward process Γ, we can conclude that

$$\langle\exp[-\Delta\Sigma]\rangle_\Gamma = \sum_f p_f^{\text{fin}}(\rho_{\text{th}}^{\text{in}}) = 1, \tag{29}$$

where we have used the fact that $p_f^{\text{fin}}(\rho_{\text{th}}^{\text{in}})$ is itself a probability distribution normalized to 1.

Description of the readout process

As described in the main text, at the end of the protocol we want to measure the probability $p_{f=1}^{\text{fin}}(\rho) \equiv \mathrm{tr}(\Pi_{f=1}^{\text{fin}}\Phi(\rho))$, where ρ is one of the four different pure states corresponding to the eigenvectors of σ_z and σ_y, and Φ is the map associated to a train of n short laser pulses ($n \in [0,N]$) with a unitary evolution U between consecutive pulses. First, the electronic spin is prepared in the desired state ρ by means of a rotation gate (on-resonant microwave pulse) to the state $|S_z = 0\rangle$. After n short laser pulses, we apply another rotation gate (on-resonant microwave pulse) such that $\tilde{\sigma}_z \to \sigma_z$. Finally, we measure the photoluminescence (PL), where the photon counts are averaged over $\sim 10^6$ repetitions of the experiment. Then, this PL intensity is normalized with respect to the reference PL intensity of the eigenstates $|S_z = 0\rangle$ and $|S_z = +1\rangle$ (also measured after each repetition of the experiment).

Let us name PL_0 and PL_1 the reference PL intensity values for the states $|S_z = 0\rangle$ and $|S_z = +1\rangle$, respectively. Thus, the normalized signal s we obtain from our experiments corresponds to $s = (PL - PL_0)/(PL_1 - PL_0)$, which is the probability to find the system in the state $|S_z = +1\rangle$. Hence, $s = \frac{1}{2}(1 + \langle\tilde{\sigma}_z\rangle) = \langle S_z = +1|\tilde{\rho}^{\text{fin}}|S_z = +1\rangle$, where $\tilde{\rho}^{\text{fin}}$ is the state of the spin qubit at the very end of the protocol. Notice though that the final rotation gate needs the change of basis $\tilde{\sigma}_z \to \sigma_z$. This rotation is described by the unitary operator $R_y(\alpha) \equiv \exp[-i\sigma_y\alpha/2]$. Therefore, $s = \langle S_z = +1|R_y(\alpha)\rho^{\text{fin}}R_y(-\alpha)|S_z = +1\rangle = \langle 1|\rho^{\text{fin}}|1\rangle$, where we have used that $R_y(-\alpha)|S_z = +1\rangle = |1\rangle$ and $\rho^{\text{fin}} = \Phi(\rho)$ is the state of the system before the final rotation. As a result, the probability that we want to measure is provided by the normalized signal $s = \mathrm{Tr}(\Phi(\rho)|1\rangle\langle 1|) = p_{f=1}^{\text{fin}}(\rho)$.

DATA AVAILABILITY

Data are available upon request from the authors.

CODE AVAILABILITY

Codes are available from the authors upon reasonable requests.

REFERENCES

1. Landi, G. T. & Paternostro, M. Irreversible entropy production: from classical to quantum. *Rev. Mod. Phys.* **93**, 035008 (2021).
2. Jarzynski, C. Nonequilibrium equality for free energy differences. *Phys. Rev. Lett.* **78**, 2690–2693 (1997).
3. Crooks, G. E. Entropy production fluctuation theorem and the nonequilibrium work relation for free energy differences. *Phys. Rev. E* **60**, 2721–2726 (1999).
4. Campisi, M., Hänggi, P. & Talkner, P. Colloquium: Quantum fluctuation relations: Foundations and applications. *Rev. Mod. Phys.* **83**, 771 (2011).
5. Esposito, M., Harbola, U. & Mukamel, S. Nonequilibrium fluctuations, fluctuation theorems, and counting statistics in quantum systems. *Rev. Mod. Phys.* **81**, 1665–1702 (2009).
6. Talkner, P., Lutz, E. & Hänggi, P. Fluctuation theorems: Work is not an observable. *Phys. Rev. E* **75**, 050102 (2007).
7. Gherardini, S., Müller, M., Trombettoni, A., Ruffo, S. & Caruso, F. Reconstructing quantum entropy production to probe irreversibility and correlations. *Quantum Sci. Technol.* **3**, 035013 (2018).
8. Manzano, G., Horowitz, J. M. & Parrondo, J. M. R. Quantum fluctuation theorems for arbitrary environments: adiabatic and nonadiabatic entropy production. *Phys. Rev. X* **8**, 031037 (2018).

9. Batalhão, T. B. et al. Experimental reconstruction of work distribution and study of fluctuation relations in a closed quantum system. *Phys. Rev. Lett.* **113**, 140601 (2014).

10. Batalhão, T. B. et al. Irreversibility and the arrow of time in a quenched quantum system. *Phys. Rev. Lett.* **115**, 190601 (2015).

11. An, S. et al. Experimental test of the quantum Jarzynski equality with a trapped-ion system. *Nat. Phys.* **11**, 193–199 (2015).

12. Smith, A. et al. Verification of the quantum nonequilibrium work relation in the presence of decoherence. *New J. Phys.* **20**, 013008 (2018).

13. Xiong, T. P. et al. Experimental verification of a jarzynski-related information-theoretic equality by a single trapped ion. *Phys. Rev. Lett.* **120**, 010601 (2018).

14. Zhang, Z. et al. Experimental demonstration of work fluctuations along a shortcut to adiabaticity with a superconducting Xmon qubit. *New J. Phys.* **20**, 085001–13 (2018).

15. Hernández-Gómez, S. et al. Experimental test of exchange fluctuation relations in an open quantum system. *Phys. Rev. Research* **2**, 023327 (2020).

16. Hernández-Gómez, S., Staudenmaier, N., Campisi, M. & Fabbri, N. Experimental test of fluctuation relations for driven open quantum systems with an NV center. *New J. Phys.* **23**, 065004 (2021).

17. Cimini, V. et al. Experimental characterization of the energetics of quantum logic gates. *npj Quantum Inf.* **6**, 1–8 (2020).

18. Ribeiro, P. H. S. et al. Experimental study of the generalized jarzynski fluctuation relation using entangled photons. *Phys. Rev. A* **101**, 052113 (2020).

19. Aguilar, G. H. et al. Two-point measurement of entropy production from the outcomes of a single experiment with correlated photon pairs. *Phys. Rev. A* **106**, L020201 (2022).

20. Allahverdyan, A. E. Nonequilibrium quantum fluctuations of work. *Phys. Rev. E* **90**, 032137 (2014).

21. Deffner, S., Paz, J. P. & Zurek, W. H. Quantum work and the thermodynamic cost of quantum measurements. *Phys. Rev. E* **94**, 010103 (2016).

22. Lostaglio, M. Quantum fluctuation theorems, contextuality, and work quasi-probabilities. *Phys. Rev. Lett.* **120**, 040602 (2018).

23. Santos, J., Celeri, L., Landi, G. & Paternostro, M. The role of quantum coherence in non-equilibrium entropy production. *npj Quantum Inf.* **5**, 23 (2019).

24. Kwon, H. & Kim, M. S. Fluctuation theorems for a quantum channel. *Phys. Rev. X* **9**, 031029 (2019).

25. Wu, K.-D. et al. Experimentally reducing the quantum measurement back action in work distributions by a collective measurement. *Sci. Adv.* **5**, eaav4944 (2019).

26. Wu, K.-D. et al. Minimizing backaction through entangled measurements. *Phys. Rev. Lett.* **125**, 210401 (2020).

27. Sone, A., Liu, Y.-X. & Cappellaro, P. Quantum jarzynski equality in open quantum systems from the one-time measurement scheme. *Phys. Rev. Lett.* **125**, 060602 (2020).

28. Micadei, K., Landi, G. T. & Lutz, E. Quantum fluctuation theorems beyond two-point measurements. *Phys. Rev. Lett.* **124**, 090602 (2020).

29. Micadei, K. et al. Experimental validation of fully quantum fluctuation theorems using dynamic Bayesian networks. *Phys. Rev. Lett.* **127**, 180603 (2021).

30. Yada, T., Yoshioka, N. & Sagawa, T. Quantum fluctuation theorem under quantum jumps with continuous measurement and feedback. *Phys. Rev. Lett.* **128**, 170601 (2022).

31. Lostaglio, M. et al. Kirkwood-dirac quasiprobability approach to quantum fluctuations: theoretical and experimental perspectives. *arXiv* https://doi.org/10.48550/arXiv.2206.11783 (2022).

32. Hernández-Gómez, S. et al. Projective measurements can probe non-classical work extraction and time-correlations. *arXiv* https://doi.org/10.48550/arXiv.2207.12960 (2022).

33. Bellini, M. et al. Demonstrating quantum microscopic reversibility using coherent states of light. *Phys. Rev. Lett.* **129**, 170604 (2022).

34. Gherardini, S., Belenchia, A., Paternostro, M. & Trombettoni, A. End-point measurement approach to assess quantum coherence in energy fluctuations. *Phys. Rev. A* **104**, L050203 (2021).

35. Hernández-Gómez, S. et al. Autonomous dissipative Maxwell's demon in a diamond spin qutrit. *PRX Quantum* **3**, 020329 (2022).

36. Maze, J. R. et al. Nanoscale magnetic sensing with an individual electronic spin in diamond. *Nature* **455**, 644 (2008).

37. Rondin, L. et al. Magnetometry with nitrogen-vacancy defects in diamond. *Rep. Prog. Phys.* **77**, 056503 (2014).

38. Degen, C. L., Reinhard, F. & Cappellaro, P. Quantum sensing. *Rev. Mod. Phys.* **89**, 035002 (2017).

39. Hernández-Gómez, S. & Fabbri, N. Quantum control for nanoscale spectroscopy with diamond nitrogen-vacancy centers: a short review. *Front. Phys.* https://doi.org/10.3389/fphy.2020.610868 (2021).

40. Crooks, G. E. Quantum operation time reversal. *Phys. Rev. A* **77**, 034101 (2008).

41. Gruber, A. et al. Scanning confocal optical microscopy and magnetic resonance on single defect centers. *Science* **276**, 2012–2014 (1997).

42. Jelezko, F., Gaebel, T., Popa, I., Gruber, A. & Wrachtrup, J. Observation of coherent oscillations in a single electron spin. *Phys. Rev. Lett.* **92**, 076401 (2004).

43. Doherty, M. W. et al. The nitrogen-vacancy colour centre in diamond. *Phys. Rep.* **528**, 1–45 (2013).

44. Aharonovich, I. & Neu, E. Diamond nanophotonics. *Adv. Opt. Mater.* **2**, 911–928 (2014).

45. Wolters, J., Strauß, M., Schoenfeld, R. S. & Benson, O. Quantum zeno phenomenon on a single solid-state spin. *Phys. Rev. A* **88**, 020101 (2013).

46. Manson, N. B., Harrison, J. P. & Sellars, M. J. Nitrogen-vacancy center in diamond: Model of the electronic structure and associated dynamics. *Phys. Rev. B* **74**, 104303 (2006).

47. Gianani, I. et al. Diagnostics of quantum-gate coherences via end-point-measurement statistics. *arXiv* https://doi.org/10.48550/arXiv.2209.02049 (2022).

AUTHOR CONTRIBUTIONS

N.F. and S.H.-G. designed and engineered the experimental protocol; S.H.-G. carried out the experiment and collected the data; S.G., A.B., A.T., and M.P. developed the theory and carried out the theoretical analysis; S.H.-G., S.G., and A.B. analyzed the data; All authors have contributed equally to the writing of the manuscript. S.H.-G., S.G., and A.B. are co-first authors.

COMPETING INTERESTS

The authors declare no competing interests.

ADDITIONAL INFORMATION

Supplementary information The online version contains supplementary material available at https://doi.org/10.1038/s41534-023-00738-0.

Correspondence and requests for materials should be addressed to Santiago Hernández-Gómez.

Reprints and permission information is available at http://www.nature.com/reprints

Publisher's note Springer Nature remains neutral with regard to jurisdictional claims in published maps and institutional affiliations.